PHYSICAL REVIEW B VOLUME 31, NUMBER 7 1 APRIL 1985

Staging: A sampling technique for the Monte Carlo evaluation of path integrals

Michiel Sprik and Michael L. Klein
Chemistry Division, National Research Council of Canada, Ottawa, Canada K1A 0R6

David Chandler
Department of Chemistry, University of Pennsylvania, Philadelphia, Pennsylvania 19104
(Received 7 November 1984)

We introduce a new sampling technique, called staging, which is likely to have applicability in the Monte Carlo evaluation of path integrals. In order to circumvent the problem of high attrition rates in the isomorphic classical system, allowed configurations are constructed with the use of a staging technique (algorithm). To illustrate the utility of this approach, the method is applied to a single quantum particle in a rigid bcc hard-sphere lattice and in a disordered system of fixed hard spheres.

I. INTRODUCTION

An important application of the path-integral formulation of quantum mechanics[1] is that it yields algorithms for the computation of equilibrium properties of quantum systems at finite temperature.[2] In particular, the isomorphism between the discretized form of the path integral and a classical system enables one to evaluate averages over the canonical ensemble for a quantum system by means of computer-simulation techniques developed for classical systems.[2] In the isomorphic classical system each quantum particle is represented by a set of classical particles arranged in a chain (the discrete path) with strong nearest-neighbor coupling.[1,2] The effective interaction between the classical particles is derived from a short-time approximation to the quantum propagator. In the lowest-order time approximation, the effective interaction is harmonic with a force constant proportional to P, the number of particles in the chain. The correspondence between the equilibrium properties of a quantum system and the isomorphic classical system is exact in the limit of infinitely large P.

The efficiency of this approach has been investigated for particles interacting via smooth model potentials (e.g., anharmonic oscillators)[3] or by means of realistic pair potentials with strong short-range repulsion.[4–9] Monte Carlo[3–7] (MC) as well as molecular-dynamics[7–9] (MD) techniques have been employed. For small systems with smooth potential surfaces accurate results can be obtained with only a limited number of chain particles ($P \approx 10$). This property of smooth potentials was exploited in a recent MC study of the structure of water where a system of 125 water molecules was employed, each with a $P=3$ discretization of the molecular orientational degrees of freedom.[10] In principle, the convergence with P could be improved by introducing more detailed effective interactions based on higher-order approximations[3] or renormalization of the propagator.[2] For steep potentials with hard cores, the convergence with P is less favorable.[4,5,11] In particular, for the extreme case of hard spheres, several hundred particles are needed when the most primitive form of the algorithm is used.[6] In this approximation, all effects of the hard cores are ignored except the excluded volume at the initial and final point of the short-time propagator. The simulation of these very large isomorphic classical systems is seriously complicated by long equilibration times. It is now appreciated that, for chains with large P, the evaluation of expectation values using MD methods is inhibited by the lack of ergodicity in the motion of the chain.[7] This situation arises because for large P the harmonic nearest-neighbor force constants are very strong compared to other interactions, and hence the normal modes of the chain are only very weakly coupled.[7] Similar problems cannot be entirely avoided by recourse to MC procedures.[6] In a straightforward implementation of the Metropolis importance sampling technique, the very stiff springs connecting two neighboring particles will allow only small amplitude displacements. Sequential chain configurations generated by moving single particles will therefore be highly correlated and long-range fluctuations will evolve only very slowly.[6]

As a solution to the convergence problem for hard-core systems, Barker proposed a modified short-time propagator which accounted for the presence of nearby boundaries of excluded volume by image terms.[12] Subsequently, Jacucci and Omerti demonstrated that for a two-body hard-sphere system, the image approximation decreased the required value of P by an order of magnitude.[6] In addition, they found that a direct MC procedure, sampling from the distribution of free harmonic chain configurations, is to be preferred. Thus, by abandoning the Metropolis scheme, the severe interdependence of the sequential configurations in the Markov chain is eliminated and the number of configurations generated can be greatly reduced.[5,6] These two features combined to yield an efficient method at least for the model two-body system (which, actually is equivalent to the problem of one particle scattered from a single hard sphere). The purpose of this paper is to examine whether the image approximation in combination with direct sampling is as useful and efficient when more than one scattering center is involved. Accordingly, we focus on a single quantum particle, described as a point mass, scattered by the hard-core potential generated by an array of hard spheres. In this pa-

per the positions of these scattering centers will be fixed either on a periodic lattice or as a disordered array. In effect, we study the equilibrium properties of a model of an electron moving in a rigid system composed of classical neutral particles.[13]

In the simulation of such a system, consisting of many scatterers, one is faced with a further difficulty related to the breakdown of ergodicity in the motion of the isomorphic string of classical particles. In both MD and MC importance sampling procedures the chain may get trapped by a local configuration composed of a few scatterers. Hence, diffusion through all of the available configuration space cannot be attained in a reasonable amount of computer time. The trapping is a consequence of the positions of the hard spheres being fixed and the fact that local fluctuations, which temporarily disrupt a chain with large P, are very unlikely to occur. The existence of many equivalent, locally stable, configurations of the chain corresponding to multiple minima in the free-energy potential is one more argument in favor of applying the direct MC procedure. However, it will be evident that at higher densities sampling from free-chain distributions becomes inefficient since the overwhelming majority of configurations generated has to be rejected because one or more of the chain's P vertices overlap with a hard sphere. While we use the hard-sphere system as a basis for discussion, the problem we have just described is much more general, and arises whenever the potential energy varies rapidly over distances much smaller than λ, the thermal wavelength of the quantum particle. As a solution to this problem we propose a modified free-chain sampling procedure, which builds up the total chain configuration in stages. The gross features of a configuration we first established using a chain with only a few particles. Then, seconary chains are inserted between adjacent vertices of the primary chain; the averages over the secondary chains determine a weight for the primary chain configuration. In this way, we are able to bypass the problem of high attrition of chain configurations generated in a system of higher density. In the next section we outline the staging algorithm. In Secs. III and IV the technique is then applied to the problem of a quantum particle which is scattered by hard spheres. First, we consider the case of one hard scatterer and then an infinite rigid lattice of hard-sphere scatterers is treated. The image approximation is reviewed. The numerical solution via the staging algorithm is substantiated by comparison to analytical solutions for these systems. The case of a disordered array of hard-sphere scatterers is studied in Sec. V. Finally, in Sec. VI both the merits and limitations of the method are summarized and possible future applications are discussed.

II. THE STAGING ALGORITHM

The equilibrium properties of a quantum particle are determined by the density matrix. The position of the quantum particle is denoted by $\mathbf{r}$ and we introduce the normalized density matrix ρ,

$$K(\mathbf{r},\mathbf{r}';\beta)=\langle \mathbf{r}\mid e^{-\beta H}\mid \mathbf{r}'\rangle = K_0(\mathbf{r},\mathbf{r}';\beta)\rho(\mathbf{r},\mathbf{r}';\beta)\ , \tag{2.1}$$

K_0 is the density matrix for the free particle,

$$K_0(\mathbf{r},\mathbf{r}';\beta)=\left[\frac{1}{2\pi\lambda^2}\right]^{3/2}\exp\left[-\frac{1}{2\lambda^2}(\mathbf{r}-\mathbf{r}')^2\right], \tag{2.2}$$

and $\lambda^2=\hbar^2\beta/m$ is the thermal wavelength. The discretized path-integral representation of K is written as

$$K(\mathbf{r},\mathbf{r}';\beta)\cong\int d\mathbf{r}_1\cdots d\mathbf{r}_{P-1}\left[\frac{P}{2\pi\lambda^2}\right]^{3P/2}\times\exp\left[-\frac{P}{2\lambda^2}\sum_{i=1}^{P}(\mathbf{r}_i-\mathbf{r}_{i-1})^2\right]\times\prod_{i=1}^{P}\tilde{\rho}(\mathbf{r}_i,\mathbf{r}_{i-1};\beta/P)\ , \tag{2.3}$$

where the path $\{\mathbf{r}_i\}$ is defined by the sequence of $P+1$ points $\mathbf{r}_0=\mathbf{r}',\ldots,\mathbf{r}_i,\ldots,\mathbf{r}_P=\mathbf{r}$; $\tilde{\rho}$ stands for the short time (high-temperature approximation) to ρ. The right-hand side of Eq. (2.3) depends on P if $\tilde{\rho}\neq\rho$ and is required to converge to the exact value on the left-hand side for $P\to\infty$. When the motion of the particle is subject to a smooth potential $V(\mathbf{r})$, it can be shown[1] that the approximation

$$\tilde{\rho}(\mathbf{r}_i,\mathbf{r}_{i-1};\beta/P)=\exp[-(\beta/P)V(\mathbf{r}_i)] \tag{2.4}$$

satisfies this requirement. For an infinitely strong repulsion the obvious choice for $\tilde{\rho}$ is to ignore the hard potential except at the $P+1$ points $\{\mathbf{r}_i\}$:

$$\tilde{\rho}(\mathbf{r}_i,\mathbf{r}_{i-1};\beta/P)=\begin{cases}1 & \text{for } |r_i|\geq d\ ,\\ 0 & \text{for } |r_i|<d\ ,\end{cases} \tag{2.5}$$

where $d=\sigma/2$ is the distance of closest approach to the center of the sphere. Approximation (2.5) is known as the primitive algorithm.[6] A formal proof of the convergence for $P\to\infty$ of the approximation (2.5) is given by Lieb.[14]

The discretization (2.3) defines an isomorphism to a classical system consisting of a chain of $P+1$ particles with constrained positions of the end points. This isomorphism is the basis for the computer evaluation of the density matrix. A straightforward implementation of such a calculation is to simulate the classical system either by MD techniques or by MC using the well-known Metropolis importance sampling. However, to avoid the serious ergodicity problems mentioned in the Introduction, we employ a direct sampling procedure which averages over independent chain configurations.[5,6] These configurations are generated according to the distribution

$$\Phi_0(\{\mathbf{r}_i\})=\left[\frac{P}{2\pi\lambda^2}\right]^{3P/2}\exp\left[-\frac{P}{2\lambda^2}\sum_{i=1}^{P}(\mathbf{r}_i-\mathbf{r}_{i-1})^2\right]\times[K_0(\mathbf{r},\mathbf{r}';\beta)]^{-1} \tag{2.6}$$

for a free chain, i.e., in absence of any external potential V. The properties of the interacting quantum particle are obtained from the reduced density matrix ρ [see Eq. (2.1)] expressed as an average with respect to Φ_0,

$$\rho(\mathbf{r},\mathbf{r}';\beta)\cong\int d\mathbf{r}_1\cdots d\mathbf{r}_{P-1}\Phi_0(\{\mathbf{r}_i\})\times\prod_{i=1}^{P}\tilde{\rho}(\mathbf{r}_i,\mathbf{r}_{i-1};\beta/P)\ . \tag{2.7}$$

A direct unbiased sampling from the distribution Φ_0 has

the important additional advantage that the free-energy difference is obtained as an average as well, since

$$\beta(F-F_0)=-\ln\left[\int d\mathbf{r}\,\rho(\mathbf{r},\mathbf{r},\beta)/V\right], \tag{2.8}$$

where F_0 is the free energy of the free particle.

As explained in the Introduction, the potential $V(r)$ must be thought of as very complicated with multiple minima corresponding to the many favored sites an electron may occupy in a classical many-body system. At low temperature the thermal wavelength is considerably larger than the distance l_V which characterizes the potential V, e.g., the average separation of these minima. This implies that the overwhelming majority of chain configurations sampled from Φ_0 in Eq. (2.6) contribute only very little to the integral (2.7). This is due to the fact that while a few particles may be in favorable position in the minima, most of the particles in the chain will be in regions of high potential energy arising from the barriers between the minima. The integral (2.7) is almost entirely determined by a very small set of configurations representing specific pathways connecting the various minima. The hard-sphere system with (2.5) provides a clear illustration of this attrition since the probability that none of the free-chain particles overlap with a hard sphere almost vanishes when the chain is very long.

The situation is not unlike the problems encountered in systems of polymers with excluded volume interaction. On the one hand, the nonergodicity of the dynamics impedes a straightforward simulation, while on the other hand, attrition makes a direct sampling procedure very inefficient. For polymers direct unbiased MC procedures have been developed which build up a full chain configuration in steps by adding particles at the end.[15,16] These algorithms are generalizations of the inverse restricted sampling technique originally designed for a self-avoiding random walk in a lattice.[15] However, these growth algorithms cannot be applied to a chain representing a path integral because of the constraints on the positions of the end points. Accordingly, we propose a different procedure. First, we establish the gross features of a chain configuration by constructing a primary chain with the correct thermal wavelength, but composed of only a few particles. Then, with the configuration of the primary chain held fixed, secondary chains are added with adjacent vertices of the primary chain as the end points. We label the primary chain with the index a and the secondary chain by b. A general configuration is described in terms of the coordinates

$$\{\mathbf{r}_i^a\}\ ,\ i=0,\ldots,P_a\ ,\quad \mathbf{r}_0^a=\mathbf{r}_{P_a}^a \tag{2.9}$$

for the a chain and

$$\{\mathbf{r}_{j,i}^b\},\ j=0,\ldots,P_b\ ,\quad i=1,\ldots,P_a\ ,$$
$$\mathbf{r}_{P_b,i}^b=\mathbf{r}_{0,i+1}^b=\mathbf{r}_i^a \tag{2.10}$$

for the P_a b chains. This configuration has P_aP_b particles. The a chain is sampled from the distribution [see Eq. (2.6)]

$$\Phi_0^a(\{\mathbf{r}_i^a\})=(2\pi\lambda^2)^{3/2}\left[\frac{P_a}{2\pi\lambda^2}\right]^{3P_a/2}\times\exp\left[-\frac{P_a}{2\lambda^2}\sum_i^{P_a}(\mathbf{r}_i^a-\mathbf{r}_{i-1}^a)^2\right]. \tag{2.11}$$

The b chains can be written as a sum of the straight classical path $\mathbf{R}$ connecting its end points and a deviation path $\Delta\mathbf{r}$:

$$\begin{aligned}&\mathbf{r}_{j,i}^b=\mathbf{R}_{j,i}^b+\Delta r_{j,i}^b\ ,\\ &\mathbf{R}_{j,i}^b=\mathbf{r}_{i-1}^a+j(\mathbf{r}_i^a-\mathbf{r}_{i-1}^a)/P_b\ ,\\ &\Delta\mathbf{r}_{0,i}^b=\Delta\mathbf{r}_{P_b,i}^b=\mathbf{0}\ ,\end{aligned} \tag{2.12}$$

with the probability for a free deviation path given by

$$\Phi_0^b(\{\Delta\mathbf{r}_{j,i}^b\})=\left[\frac{2\pi\lambda^2}{P_a}\right]^{3/2}\left[\frac{P_aP_b}{2\pi\lambda^2}\right]^{3P_aP_b/2}\times\exp\left[-\frac{P_aP_b}{2\lambda^2}\sum_{j=1}^{P_b}(\Delta\mathbf{r}_{j,i}^b-\Delta\mathbf{r}_{j-1,i}^b)^2\right]. \tag{2.13}$$

The advantage of first setting down a large scale primary chain is twofold. First, the primary chain consisting of only a few particles provides us with a simple rough estimate of W, the weight of the full chain in the integral (2.7)

$$W=\exp\left[-\frac{\beta}{P_a}\sum_{i=1}^{P_a}V(\mathbf{r}_i^a)\right]. \tag{2.14}$$

This number can be used as a criterion to decide whether to continue building up the chain by inserting the second stage or to reject the configuration because its weight will be negligible. The criterion for rejection is particularly simple for hard-core interactions. Overlap of one or more of the chain particles in the primary chain sets the full weight to zero. If P_a is sufficiently small the probability of generating a primary chain, which violates the excluded volume condition, can be reduced to a minimum. Equally important is the fact that the average separation between the particles in the a chain is of the same order as l_V. This feature ensures that the probability of generating a chain with vertices located in different minima is finite, thus avoiding the problem of being trapped in one minimum. The energy barriers between minima are then accounted for by the weights of the secondary chains. For an accurate estimation of these weights the insertion of secondary b chains must be repeated many times for one fixed a-chain configuration. From this staging procedure the following estimator for the integral (2.7) is obtained:

$$\begin{aligned}&\bar\rho(\mathbf{r},\mathbf{r}')=\frac{1}{N_G^a}\sum\prod_{i=1}^{P_a}\bar\rho^{\,b}(\mathbf{r}_i^a,\mathbf{r}_{i-1}^a;\beta/P_a)\ ,\\ &\bar\rho^{\,b}(\mathbf{r}_i^a,\mathbf{r}_{i-1}^a;\beta/P_a)=\frac{1}{N_{Gi}^b}\sum\prod_{j=1}^{P_b}\tilde\rho(\mathbf{r}_{j,i}^b,\mathbf{r}_{j-1,i}^b;\beta/P_aP_b)\ ,\end{aligned} \tag{2.15}$$

where the first summation is over the N_G^a primary chain

configurations sampled from the distribution (2.11) and the second summation is over the N^b_{Gi} secondary chain configurations inserted at the link i of the a chain according to (2.12) and (2.13). This approach is justified by the fact that the probability density for the full path of the free particle factorizes into a product of the distribution functions defined above. This follows if Eq. (2.12) is substituted into the expression for the full action S,

$$S=\frac{P_aP_b}{2\lambda^2}\sum_{i=1}^{P_a}\sum_{j=1}^{P_b}(\mathbf{r}^b_{j,i}-\mathbf{r}^b_{j-1,i})^2$$
$$=\frac{P_aP_b}{2\lambda^2}\sum_{i=1}^{P_a}\sum_{j=1}^{P_b}\left[\frac{1}{P_b^2}(\mathbf{r}^a_i-\mathbf{r}^a_{i-1})^2+(\Delta\mathbf{r}^b_{j,i}-\Delta\mathbf{r}^b_{j-1,i})^2+\frac{2}{P_b}(\mathbf{r}^a_i-\mathbf{r}^a_{i-1})\cdot(\Delta\mathbf{r}^b_{j,i}-\Delta\mathbf{r}^b_{j-1,i})\right]. \tag{2.16}$$

Upon summation over the index j we find that the cross term vanishes because of the boundary condition of Eq. (2.12) for $\Delta\mathbf{r}^b$, and hence

$$S=\frac{P_a}{2\lambda^2}\sum_{i=1}^{P_a}(\mathbf{r}^a_i-\mathbf{r}^a_{i-1})^2+\frac{P_aP_b}{2\lambda^2}\sum_{i=1}^{P_a}\sum_{j=1}^{P_b}(\Delta\mathbf{r}^b_{j,i}-\Delta\mathbf{r}^b_{j-1,i})^2 . \tag{2.17}$$

Similarly, the normalization factor of the distribution Φ_0 separates in a product of the normalization factors in Eqs. (2.11) and (2.13), and therefore

$$\Phi_0(\{\mathbf{r}^b_{j,i}\})=\Phi^a_0(\{\mathbf{r}^a_i\})\prod_{i=1}^{P_a}\Phi^b_0(\{\Delta\mathbf{r}^b_{j,i}\}) . \tag{2.18}$$

Insertion of (2.18) into expression (2.7) yields a superposition relation for the density matrix

$$\rho(\mathbf{r},\mathbf{r}';\beta)\cong\int d\mathbf{r}^a_1\cdots d\mathbf{r}^a_{P_a-1}\Phi^a_0(\{\mathbf{r}^a_i\})\times\prod_{i=1}^{P_a}\tilde{\rho}^b(\mathbf{r}^a_i,\mathbf{r}^a_{i-1};\beta/P_a) ,$$
$$\tilde{\rho}^b(\mathbf{r}^a_i,\mathbf{r}^a_{i-1};\beta/P_a)=\int d\Delta\mathbf{r}^b_{1,i}\cdots d\Delta\mathbf{r}^b_{P_b-1,i}\Phi^b_0(\{\Delta\mathbf{r}^b_{j,i}\})\times\prod_{j=1}^{P_b}\bar{\rho}(\mathbf{r}^b_{j,i},\mathbf{r}^b_{j-1,i};\beta/P_aP_b) . \tag{2.19}$$

In Eq. (2.19) the integration over the variables $\mathbf{r}_{j,i}, j=1,\ldots,P_b-1$ has been replaced by the integration over the coordinates of the deviation path. The quantity $\tilde{\rho}^b$ may be considered as a renormalized weight for an elementary path in the a chain and will converge to the true weight for $P_b\to\infty$. The right-hand side (rhs) of Eq. (2.15) converges in the limit of an infinite number of sample configurations ($N^a_G, N^b_{G,i}\to\infty$) to the rhs of Eq. (2.19), from which we conclude that $\bar{\rho}$ in Eq. (2.15) is a valid estimator of ρ. At lower temperatures or for potentials corresponding to dense systems it will be necessary to repeat the staging procedure and insert third-order chain configurations between the vertices of the second-order chains. The expression for $\bar{\rho}$ can be obtained by iteration of Eq. (2.15).

III. SCATTERING FROM HARD SPHERES

A quantum particle moving in a potential which consists of fixed uncharged hard spheres[13] provides a suitable problem to illustrate the use of staging. If the high-temperature propagator $\tilde{\rho}$ is approximated by Eq. (2.5), an estimate of ρ can be obtained from acceptance ratios in the direct sampling procedure. This result follows immediately from Eq. (2.7), when no staging is applied.[6] If out of a sample of N_G configurations $\{\mathbf{r}_i\}$, generated according to the distribution Φ_0, N_A configurations do not overlap at any of the $P+1$ points with a hard sphere, then

$$\bar{\rho}(\mathbf{r},\mathbf{r}';\beta)\cong\frac{N_A(P)}{N_G} . \tag{3.1}$$

A sample of N_G independent free-particle chains, all starting at $\mathbf{r}_0=\mathbf{r}$ and ending at $\mathbf{r}_P=\mathbf{r}$, can be constructed from $3N_G(P-1)$ independent Gaussian random variables using a method based on the Levi interpolation formula for the conditional Wiener path.[6] However, in the present work we prefer to use the normal-mode coordinates of a harmonic chain with fixed end points as the independent Gaussian variables.[7] The width of the Gaussian distribution for a normal-mode amplitude is inversely proportional to its frequency. The phases are uniformly distributed. A configuration in real space is then obtained by an inverse Fourier transform. This approach is different from that employed in Ref. 17 where the continuous path is resolved in Fourier components.

In Ref. 6 the efficiency of the direct sampling algorithm was investigated by comparing the resulting estimates for the pair correlation function for two hard spheres to exact values obtained from a partial-wave expansion.[18] The pair correlation function for two identical particles can be written as a sum of a direct part g_d and an exchange part g_e.[6,18] If the mass of each particle is $2m$, then g_e is related to ρ in definition (2.1) by the equation

$$g_e(r)=\exp\left[-2\frac{r^2}{\lambda^2}\right]\rho(\mathbf{r},-\mathbf{r};\beta) , \tag{3.2}$$

where r is the relative coordinate. Figure 1 gives the result for g_e for one particular distance close to the boundary of excluded volume. The thermal wavelength corresponds to the value of the lowest temperature investigated in Refs. 6 and 18. The data for small values of P have been obtained by means of the one-stage algorithm (3.1) and agree with the results of Ref. 6. For large P they have been determined using the two-stage approximation

$$\bar{\rho}(\mathbf{r},\mathbf{r}',\beta)=\frac{1}{N_G^a}\sum\prod_{i=1}^{P_a}\frac{N_{A,i}^b}{N_{G,i}^b}\ . \tag{3.3}$$

The estimator (3.3) is derived from the general expression (2.15) when the primitive approximation (3.1) is substituted for the propagator $\bar{\rho}^b(\mathbf{r}_i^a,\mathbf{r}_{i-1}^a;\beta/P_a)$. Now $N_{G,i}^b$ is the total number of trial b-chain configurations added between the vertex $\mathbf{r}_{i-1}^a$ and $\mathbf{r}_i^a$, and $N_{A,i}^b$ is the number of configurations in this set which do not overlap with a hard sphere. The results of the second-order staging procedure are in good agreement with those of (3.1), provided that the number of accepted secondary chains per particle in the fixed a chain is sufficiently large ($N_{A,i}^b>50$). Sets of b-chain configurations for which the acceptance ratio is determined in order to estimate the renormalized propagator $\bar{\rho}^b$ [see Eq. (2.15)] between a-chain vertices, are not required to be independent. Hence, the same sample of deviation path configurations can be used for all a-chain links. In this way a considerable reduction of computer time can be achieved, and the checking for overlap with hard spheres becomes the most time-consuming process. Also indicated in Fig. 1 is the exact value of g_e derived from a partial-wave expansion.[18] Clearly, the convergence with P is disappointing, particularly since the thermal wavelength in Fig. 1 is typical of helium atoms at low temperature and therefore comparable to an electron at much higher temperature. However, the number of chain particles, P can be dramatically reduced if the image approximation is used for ρ:[6,12]

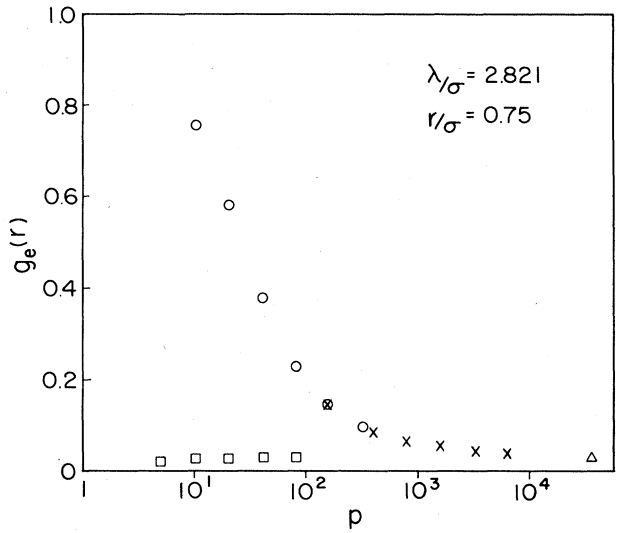

FIG. 1. Exchange part of the pair correlation function $g_e(r)$, for two identical particles at fixed separation r, as a function of the number of particles P in the chain. The definition of thermal wavelength and separation refer to a point mass m scattered from a hard sphere with radius $d=\sigma/2$ (see Sec. III). Open circles and crosses indicate estimates obtained in the primitive approximation (2.5) with use of, respectively, one- and two-stage sampling. Squares indicate estimates obtained in the image approximation (3.4) with use of one-stage sampling. The triangle is the exact value given in Ref. 18.

$$\tilde{\rho}(\mathbf{r}_i,\mathbf{r}_{i-1};\beta/P)=\begin{cases}\left[1-\exp\left[-\dfrac{2P}{\lambda^2}(|r_i|-d)(|r_{i-1}|-d)\right]\right] & \text{if } |\mathbf{r}_i|,|\mathbf{r}_{i-1}|\geq d\ ,\\ 0, \text{ otherwise}\ .\end{cases} \tag{3.4}$$

In Eq. (3.4) the value of $\tilde{\rho}$ is forced to zero at the boundary of the excluded volume by subtracting the propagator of an oblique path reflected by the surface of the sphere.[12] In this approximation the estimate of ρ is no longer obtained as an acceptance ratio (3.1). Instead, the average of a product of factors (3.4) should be evaluated.[6,12] However, ρ can still be formally interpreted as an acceptance ratio. The results of the one-stage image approximation are compared to the primitive algorithm in Fig. 1.

While the attrition for the case of an electron scattering from a single hard sphere (Fig. 1) is still not too serious as to prohibit the use of a direct one-stage procedure, this is no longer true when additional hard spheres are present. The attrition can be interpreted as a free-energy difference with respect to a free quantum particle. This relation is made explicit when the primitive approximation (3.1) for ρ is substituted in Eq. (2.8), giving us

$$\beta(F-F_0)=-\ln[N_A(P)/N_G]\ . \tag{3.5}$$

In Eq. (3.5) the acceptance ratio is to be determined from a sample of free chains with the end points identified ($\mathbf{r}_0=\mathbf{r}_P$) and no longer fixed at one point $\mathbf{r}$ in the system. As explained above, we perform the averaging by sam-

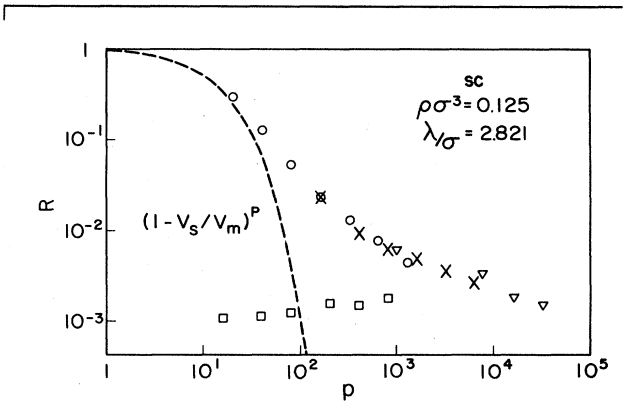

FIG. 2. Convergence with the number of particles in the chain P for the (effective) acceptance ratio R, in a simple-cubic lattice of hard spheres. The thermal wavelength λ is the same as in Fig. 1. Circles, crosses, and triangles indicate estimates obtained in the primitive approximation (2.5) with use of, respectively, one-, two-, and three-stage sampling. Squares indicate estimates obtained in the image approximation (3.6) with use of two-stage sampling. The dashed curve is the acceptance ratio for independent particles determined by the volume per hard sphere V_m and the volume of a hard sphere V_s.

pling the normal-mode coordinates of the free chain. Since in Eq. (3.5) there are no constraints on the position of the end point $\mathbf{r}$, the normal modes are most conveniently represented by their amplitudes and phases. The normal-mode sampling has the additional advantage that the center of mass of the chain is treated as an independent random variable, namely the zero wave-vector ($\mathbf{k}=0$) mode. In this way we can confine the center of mass to a restricted volume and avoid imposing any other volume constraint on the remaining chain coordinates. In Fig. 2 we show the calculated acceptance ratio $R=N_A/N_G$ as a function of P for an electron in a simple cubic (sc) lattice of hard spheres. The sc bravais lattice was constructed by periodically replicating one sphere and hence all boundaries in the system are eliminated. The c.m. is integrated over one lattice cell (see also Sec. V). The density of hard spheres ($\rho\sigma^3=0.125$) is low and is actually more characteristic for a gas than a solid. For purpose of comparison to the case of one scatterer we have used a $\lambda/\sigma=2.82$, which is the same value as in Fig. 1. The acceptance ratio R decreases rapidly with increasing P and more than 10^4 particles are needed to obtain the asymptotic value of about one accepted configuration out of 1000 attempts. The results for the smallest values of P in Fig. 2 were determined using the one-stage algorithm of Eq. (3.5). For the intermediate values of P a two-stage procedure was applied, while the longest chains were constructed in three stages. The appropriate expressions for the estimator of the free energy are easily derived from Eqs. (2.8) and (2.15).

The attrition rate escalates rapidly with increasing density or thermal wavelength and proper convergence in the primitive algorithm would require a chain with a prohibitively large number of particles. Instead, we have employed an extension of the image approximation which takes account of the excluded volume of more than one hard sphere in combination with a staging procedure for building up the chain. The expression (2.15), which gives an estimate for ρ, is equally valid when the image approximation is applied to modify the propagator between the nearest-neighbor vertices in the chain of the last stage (the one with the smallest λ^2/P). However, since now the scattering occurs from more than one hard sphere, the expression (3.4) has to be adapted accordingly. A simple extension of Eq. (3.4), which takes into account only two special spheres, is

$$\tilde{\rho}(\mathbf{r}_i,\mathbf{r}_{i-1};\beta/P)=\left[1-\exp\left[-\frac{2P}{\lambda^2}(|\mathbf{r}_i-\mathbf{R}_i|-d)(|\mathbf{r}_{i-1}-\mathbf{R}_i|-d)\right]\right]\times\left[1-\exp\left[-\frac{2P}{\lambda^2}(|\mathbf{r}_i-\mathbf{R}_{i-1}|-d)(|\mathbf{r}_{i-1}-\mathbf{R}_{i-1}|-d)\right]\right] \tag{3.6}$$

with

$$\mathbf{R}_i\neq\mathbf{R}_{i-1}\ ,$$

where $\mathbf{R}_{i-1}$ and $\mathbf{R}_i$ are the spheres closest to the initial point $\mathbf{r}_{i-1}$ and the final point $\mathbf{r}_i$, respectively. When these spheres turn out to be the same, the second factor is omitted and the expression (3.6) reduces to Eq. (3.4). Clearly, the propagator is an approximation justified in the limit where $\lambda/\sqrt{P}$ is sufficiently smaller than the average distance between the spheres. It was found that in this definition the image approximation is most efficient when about half of the links $(\mathbf{r}_i,\mathbf{r}_{i-1})$ have separate spheres closest to their initial and final point. While it is possible to include more detailed features of the environment of a set of points $(\mathbf{r}_i,\mathbf{r}_{i-1})$, this has not been investigated. The results of the image approximation for the sc lattice are compared to the primitive algorithm in Fig. 2. The improvement in the convergence with P is even more marked than for the case of scattering from one sphere shown in Fig. 1. It should be recalled, however, that the presence of more than one hard sphere implies various additional tasks for the algorithm such as sorting distances.

A study of the temperature dependence of the attrition rate in a lattice provides us with a powerful test of the algorithm. In a hard-sphere system the free energy is a direct measure of the attrition. Therefore, it can be expected that the free energy will increase when the temperature is reduced. However, despite the high attrition rate, the eigenstates of the quantum particle retain an extended quasi free character because of the translation symmetry of the lattice (Bloch theorem). Figure 3 shows the free-energy difference $\beta(F-F_0)$ as a function of P for a body-centered-cubic lattice of hard spheres of density $\rho\sigma^3=0.25$ at various temperatures. The thermal wavelengths are all considerably larger than the lattice parameter, and a sphere defined by the radius of gyration of the chain typically contains about 10 hard spheres at the higher temperatures in Fig. 3 and about 100 hard spheres at the lower temperatures. To generate the data shown in Fig. 3 both second-order and third-order staging has been applied in combination with the image approximation (3.6). The asymptotic values at large P are plotted as a function of $\lambda^2\sim\beta$ in the inset of Fig. 3. The observed linear dependence of $\beta(F-F_0)$ on λ^2 is a direct consequence of the quasi free character of the states available to the quantum particle.

In the long-wavelength limit the energy eigenvalue of a state with wave vector k can be approximated as

$$E(k)\cong E(\Gamma)+\hbar^2k^2/2m^*\ , \tag{3.7}$$

where m^* is the effective mass. $E(\Gamma)$ is the energy at the Brillouin-zone center, Γ, and is positive for a lattice of hard spheres. The approximation (3.7) yields a free energy

$$\beta(F-F_0)=\beta E(\Gamma)-\tfrac{3}{2}\ln(m^*/m)\ . \tag{3.8}$$

In a system of relatively low density we may assume that $m^*\approx m$. The first term in (3.8) will dominate, explaining

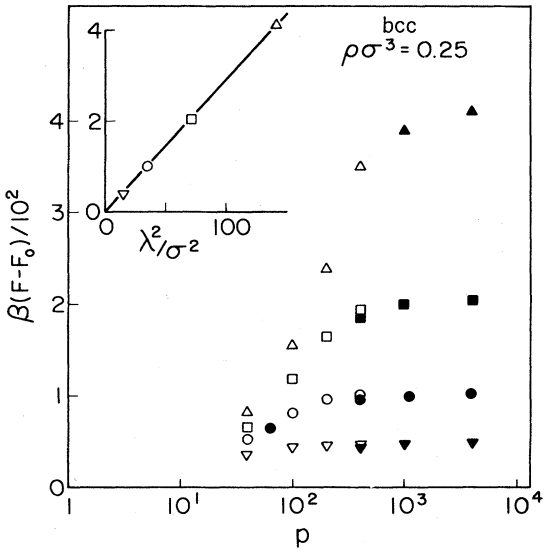

FIG. 3. The free-energy difference between a quantum particle confined to a lattice of hard spheres and a free particle as a function of the number of particles in the chain, P. Inverted triangles, circles, squares, and triangles indicate estimates for $\lambda/\sigma=4.0$, 6.0, 8.4, and 11.9, respectively. Open symbols denote results obtained by means of the image approximation with use of two-stage sampling; solid symbols are for three-stage results. The inset shows the temperature dependence of the converged values in the same units as the main figure.

the λ^2 dependence observed in Fig. 3. The band-edge energy $E(\Gamma)$ can be calculated using one of the methods of solid-state theory. For a lattice of hard spheres the Wigner-Seitz[19] model is particularly suitable. Within this model $E(\Gamma)=\hbar^2k^2/2m$, where k is determined from

$$\tan[k(r_s-d)]=kr_s \ , \quad \text{where} \quad \tfrac{4}{3}\pi(r_s/\sigma)^3=(\rho\sigma^3)^{-1} \ . \tag{3.9}$$

If we substitute the parameters of Fig. 3 into (3.9) we find for $E(\Gamma)=2.97$ in units $\hbar^2/m\sigma^2$, which is in good agreement with the value 2.90 determined from the slope in Fig. 3. We therefore conclude that we can adequately simulate a delocalized electron in a low-density system of scatterers using the staging algorithm.

IV. STRUCTURE AND KINETIC ENERGY

Structural properties such as correlation functions are most efficiently evaluated by including only the particles of the primary stage (the a chain) in the averaging. In this way, the time-consuming accumulation of averages over secondary chain configurations can be avoided. If $A(\{\mathbf{r}_i^a\})$ denotes a function defined on the a chain configuration, the average of A is given by

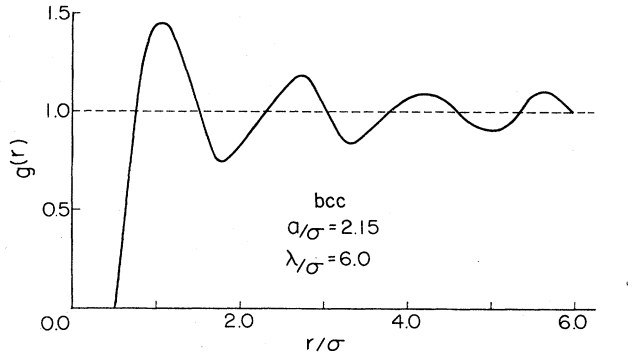

FIG. 4. The quantum-particle—hard-sphere radial distribution function $g(r)$ in a bcc lattice of hard spheres of density $\rho\sigma^3=0.201$ and $\lambda/\sigma=6.0$.

$$\langle A\rangle=\frac{1}{Z}\int d\mathbf{r}_1\cdots d\mathbf{r}_{P_a} A(\{\mathbf{r}_i^a\})\Phi_0(\{\mathbf{r}_i^a\}) \times\prod_{i=1}^{P_a}\bar{\rho}^{\,b}(\mathbf{r}_i^a,\mathbf{r}_{i-1}^a;\beta/P_a) \ , \qquad Z=e^{-\beta(F-F_0)} \ . \tag{4.1}$$

For the two-stage procedure, the quantity $\bar{\rho}^{\,b}$ is given in Eq. (2.15). Figure 4 shows the electron lattice correlation function for a bcc lattice with $\rho\sigma^3=0.2$. The maximum of the first peak is located at a distance which is slightly larger than half the lattice parameter of the cubic unit cell ($a/\sigma=2.15$). This suggests that the vacant sites (both tetrahedral and octahedral) at the center of the faces of the cubic unit cell are preferred locations for the electron. A measure of the extension of the thermal wave packet of the electron is given by the rms relative displacement at half the chain length. This quantity can be expressed as an average over the chain particle positions as

$$r_{1/2}\cong\left[\frac{1}{P_a}\left\langle\sum_{i=1}^{P_a}(\mathbf{r}_{i+P_a/2}^a-\mathbf{r}_i^a)^2\right\rangle\right]^{1/2} \ , \tag{4.2}$$

where the average is determined according to Eq. (4.1). If the average is evaluated with respect to the Boltzmann distribution related to the energy spectrum (3.7), $r_{1/2}$ for a quasi free electron is found to be

$$r_{1/2}=\tfrac{1}{2}\sqrt{3}(m/m^*)^{1/2}\lambda \ . \tag{4.3}$$

As is shown in Fig. 5, the electron in a low-density bcc lattice is only slightly less extended than a completely free electron. The discrepancy can be explained by the particle being effectively heavier in the lattice ($m^*>m$).

Unlike structural properties the kinetic energy cannot be determined from the coordinates of the particles in the primary chain only. This is a consequence of the fact that the kinetic operator is a differential operator. For a system with infinitely hard potentials the kinetic energy is related to the free energy by means of a derivative with respect to temperature. Hence employing Eq. (2.8), we can write[12]

$$E=-\frac{1}{Z}\int d\mathbf{r}_1\cdots d\mathbf{r}_p\Phi(\{\mathbf{r}_i\})\frac{d}{d\beta}\ln[(2\pi\lambda^2)^{-3/2}\times\Phi(\{\mathbf{r}_i\})]\,, \tag{4.4}$$

$$\Phi(\{\mathbf{r}_i\})=\Phi_0(\{\mathbf{r}_i\})\prod_{i=1}^{P}\tilde{\rho}(\mathbf{r}_i,\mathbf{r}_{i-1};\beta/P)\,.$$

This implies that the kinetic energy consists of a contribution E_0 due to the free-chain distribution P_0 and a contribution $\tilde{E}$ arising from the particular approximation used for $\tilde{\rho}$:[12]

$$E=E_0+\tilde{E}\,,$$
$$\beta E_0=\tfrac{3}{2}P\left[1-\frac{1}{3\lambda^2}\left\langle\sum_{i=1}^{P}(\mathbf{r}_i-\mathbf{r}_{i-1})^2\right\rangle\right]\,, \tag{4.5}$$
$$\tilde{E}=-\left\langle\sum_{i=1}^{P}\frac{\partial}{\partial\beta}\ln\tilde{\rho}(\mathbf{r}_i,\mathbf{r}_{i-1};\beta/P)\right\rangle\,.$$

The angular brackets denote an average with respect to the full distribution Φ defined in Eq. (4.4). For the case of second-order staging E_0 can be resolved into a-chain coordinates and b-chain deviation-path coordinates by means of Eq. (2.17):

$$\beta E_0=\tfrac{3}{2}P_aP_b\left[1-\frac{1}{3\lambda^2}\left\langle\frac{1}{P_b}\sum_{i=1}^{P_a}(\mathbf{r}_i^a-\mathbf{r}_{i-1}^a)^2+\sum_{i=1}^{P_a}\sum_{j=1}^{P_b}(\Delta\mathbf{r}_{j,i}^b-\Delta\mathbf{r}_{j-1,i}^b)^2\right\rangle\right]\,. \tag{4.6}$$

The $\tilde{E}$ term is determined by the propagator connecting the vertices of the b chains:

$$\tilde{E}=-\sum_{i=1}^{P_a}\left\langle\sum_{j=1}^{P_b}\frac{\partial}{\partial\beta}\ln\tilde{\rho}(\mathbf{r}_{j,i}^b,\mathbf{r}_{j-1,i}^b;\beta/P_aP_b)\right\rangle\,. \tag{4.7}$$

For the primitive approximation (2.5) $\tilde{E}$ vanishes. However, for the image approximation (3.6), $\tilde{E}$ is finite and turns out to be the dominant contribution to the total kinetic energy. We also note that in a lattice, because of Eqs. (3.7) and (3.8), when $m^*>m$ the following inequality holds:

$$F-F_0<E\,. \tag{4.8}$$

This relation can be employed to test the consistency of the actual implementation of an algorithm. In Fig. 6 the kinetic energy is compared to the free energy for the bcc lattice for $\lambda/\sigma=6.0$ and various densities. The inequality (4.8) is satisfied at all density points in Fig. 6. At higher density, E is only marginally larger than $F-F_0$, since both quantities are dominated by the very-high band-edge energy $E(\Gamma)$ [see Eq. (3.7)].

V. THE RIGID DISORDERED SYSTEM

When the condition of periodicity of the hard spheres is relaxed, several of the simplifications in the staging algorithm discussed in the preceding sections are no longer valid. For the lattice the averages were performed by constructing the hard-sphere environment for each pair of neighboring vertices, for which the violation of excluded volume is investigated and to which the image approximation (3.6) is applied. This environment is the image under

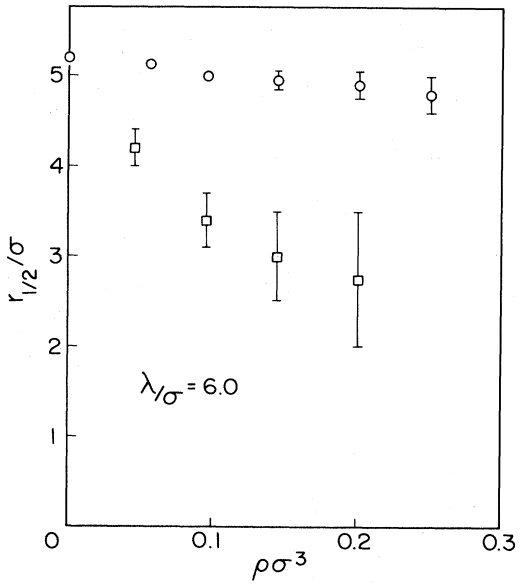

FIG. 5. The root-mean-square displacement at half the chain length [Eq. (4.2)] as a function of density. Circles and squares indicate, respectively, averages over a bcc lattice and a rigid disordered system of hard spheres.

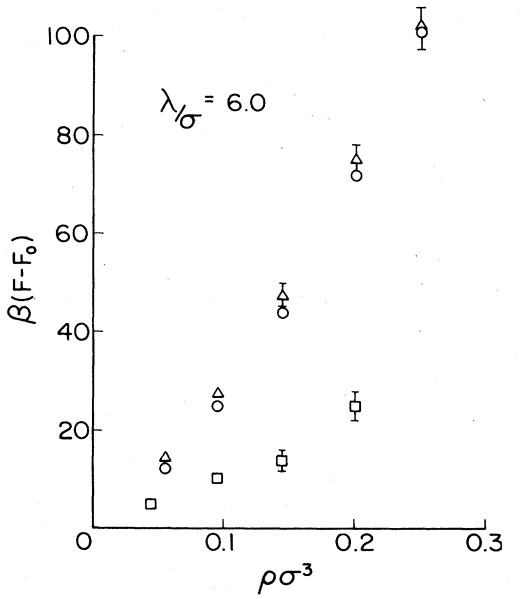

FIG. 6. Free-energy difference with respect to the free-particle limit as a function of density for a quantum particle in a bcc lattice of hard spheres (circles) and a rigid disordered system of hard spheres (squares). Triangles indicate E, the average kinetic energy for the particle in the lattice (see Sec. IV).

the lattice symmetry operations of a set of adjacent unit cells at the origin with the properties that the chain particles considered are in this image. This replication procedure cannot be used in a disordered system where the positions of the hard-sphere scatterers are no longer related by symmetry. Now, the chain particles have to be inserted into a sufficiently large but finite system of fixed hard spheres. This implies that the position of a chain particle has to be compared to the coordinates of a much larger number of spheres. For the secondary chains this task can be reduced to a considerable extent by the construction of maps of the environment of each link in the primary chain (a-chain neighbor lists). When the primary chain configuration is generated and the coordinates of all the spheres are investigated a list is made of all the spheres in the vicinity of a pair of adjacent vertices. This environment is chosen sufficiently large to contain the majority of possible b-chain configurations fitted between the two a-chain vertices. Then in the process of averaging over the secondary chain configuration [see Eq. (2.15)] only the spheres in this set have to be considered. A convenient shape for such an environment is an ellipsoid with the two a-chain vertices as foci and a minor axis determined by $\lambda/\sqrt{P_a}$ and the hard-sphere radius d.

A second complication due to the disorder is the introduction of boundaries. The replication procedure described above effectively extends the lattice to infinity. The disordered system, however, has a finite dimension. In the present calculation the hard spheres are inside a volume with the shape of a truncated octahedron. The distribution of spheres is generated by a MC program for hard spheres with the truncated octahedron as a periodic boundary.[20] Once a configuration of the hard spheres is selected, the staging algorithm, which averages over chain configurations, is applied without periodic boundaries. Instead, the coordinates of the center of mass of the chain (c.m.) are constrained to a smaller cube at the center of the octahedron. The system of hard spheres, therefore, should be sufficiently large in order that the majority of the generated chain configurations has no vertices outside the octahedron. The size of the outer octahedron is therefore determined by both the extension of the free chain and the volume of the inner cube. In actual calculations the dimension of the outer octahedron for a given density of hard spheres is chosen sufficiently large to reproduce the results obtained for the periodic lattice by means of the replication procedure.

The criteria for choosing the dimensions of the inner cube, which contains the center of mass of the chain (i.e., the zero-frequency component of the path) are less unambiguous and depend upon whether the averages over hard-sphere configurations are performed as annealed or quenched averages. For example, it follows from ergodicity arguments that the equilibrium properties of a quantum particle in an infinitely large disordered system of fixed hard spheres are identical to the annealed averages which are obtained by removing the constraints on the positions of the hard spheres.

Let us denote the configuration of the spheres in the outer octahedron by the symbol κ. We will consider an assembly of many κ, and imagine that this assembly was formed by subdividing a single huge disordered system into many truncated octahedra. In this picture the inner cubic cell simply confines the quantum particle to a region of space, allowing it to sample an environment characterized by the configuration κ. For each fixed κ, the sampling of chain configurations via the staging algorithm yields a partition function

$$Z_\kappa = \exp[-\beta(F_\kappa - F_0)] , \tag{5.1}$$

where F_κ denotes the free energy (or chemical potential) for the quantum particle confined to the inner cube in the octahedron with a random hard-sphere configuration. It is straightforward to show that in the limit of a very large number of uncorrelated configurations, the sum of these partition functions,

$$Z = \sum_\kappa Z_\kappa , \tag{5.2}$$

is the partition function for the annealed, i.e., thermally equilibrated, system. In particular, $\ln Z$ is the generating functional for the averages

$$\langle A \rangle = \sum_\kappa \langle A \rangle_\kappa \exp[-\beta(F_\kappa - F_0)]/Z , \tag{5.3}$$

which are averages Boltzmann weighted by the individual free energies F_κ. It also can be shown that such partitioning and averages are independent of the size of the inner cube (provided that it remains much smaller than the octahedron).

This invariance does not carry over, however, to the case of quenched averages. Here, the particular size of the inner cube should be chosen with due regard for the particular experimental probe one has in mind. Once a choice is made for this partitioning, the appropriate quenched averages, for a frozen disordered material, are unbiased by the free energies F_κ, and are given by

$$\langle A \rangle_q = \frac{1}{n} \sum_{\kappa=1}^{n} \langle A \rangle_\kappa , \tag{5.4}$$

where n is the number of different sampled configurations. The subscript q indicates a quenched average. Its generating functional is

$$\ln Z_q = \frac{1}{n} \sum_{\kappa=1}^{n} \ln Z_\kappa . \tag{5.5}$$

Since we lack an unambiguous criterion for carrying out the partitioning required for a quenched average (5.4), we have only presented results obtained using the Boltzmann weighted average (5.3). Figures 5 and 6 contain our estimates $r_{1/2}$ [recall Eq. (4.2)] and the free energy for a quantum particle in a rigid disordered system of hard spheres. For comparison, the corresponding values in a bcc lattice are also shown. The annealed averages were evaluated from (5.2) and (5.3) by combining the results of about 100 independent hard-sphere distributions. For each configuration of hard spheres, the c.m. of the chain was confined to a volume containing about 15 hard spheres. At the density $\rho\sigma^3 = 0.2$ averages determined from a set of such calculations agree, within fairly large statistical errors, with the results obtained by randomly

TABLE I. (a) Convergence characteristics for properties of a quantum particle with the mass of an electron in a fixed disordered configuration of hard spheres. Averages are obtained by means of the two-stage sampling procedure and the image approximation. P_a and N_G^a denote, respectively, the number of particles in the primary chain and the number of generated primary chain configurations. P_b and $N_{G,i}^b$ denote, respectively, the number of particles in a secondary chain and the number of secondary chain configurations generated per primary chain configurations. (b) Sample characteristics for the data in (a). (Length is expressed in units of the hard-sphere diameter σ.)

(a)

P_aP_b	$N_G^a/10^3$	$N_{G,i}^b$	$\beta(F-F_0)$	$r_{1/2}$
8×8	62	100	21.9	2.5
16×8	102	100	23.4	3.13
16×16	140	100	25.0	3.14
16×32	39	400	25.3	3.33

(b)

Number of hard spheres	2197
Length of cube edge defining the truncated octahedron	27.95
Density, $\rho\sigma^3$	0.201
Thermal wavelength of quantum particle, λ/σ	6.0
Length of cube edge containing c.m. of chain	6.45

sampling the c.m. of the chain from a volume containing about 50 hard spheres (see Table I). The convergence characteristics of the latter calculation, which was based on a two-stage algorithm, are also listed in Table I. It is clear from Figs. 5 and 6 that the properties of a quantum particle in a disordered system differ significantly from those in a lattice; the free energy is about 3 times lower in the disordered system and the quantum particle is considerably more localized. This phenomenon can be explained by the importance of local-density fluctuations in the disordered system. As is evident from Fig. 5, the free energy shows a strong increase with density. The chain particles will therefore concentrate in regions with relatively few hard spheres, thus reducing the free energy, and as a consequence the average chain configuration will be compressed. This effect is also the main reason for the averages in the disordered system being less accurate in comparison to those for the lattice, since they are dominated by the infrequently generated, preferred primary chain configurations with high weights. As a consequence, the data in Figs. 5 and 6 are based upon relatively few configurations and therefore cannot be considered as fully converged annealed averages. For a study of the fully annealed system a procedure where the spheres are allowed to relax in response to the presence of the quantum particle would seem to be more appropriate.

VI. DISCUSSION

The staging algorithm introduced in this paper has been developed for the specific purpose of evaluating path sums in systems which are difficult to simulate by conventional MD and MC methods because of the importance of both fluctuations and attrition effects. The potential-energy surface for the quantum particle has a complicated structure with many minima separated by large barriers, as is characteristic for an electron in a delocalized state in a solid or fluid. As mentioned in Sec. II, the problems besetting an evaluation of path sums in such a system are very similar to those encountered in a simulation of polymers with excluded volume interaction. In fact, the staging algorithm, which we propose, might also prove useful in the averaging over polymer configurations.

A further important extension is the possibility of removing the constraint of a rigid potential by allowing the classical particles, which interact with the quantum particle, to adapt to the presence of the quantum particle. One way to implement this annealing procedure is to determine first the free energy of the quantum particle, by the staging algorithm for fixed coordinates of the center of mass of the chain and fixed position of the classical particles. Then, the coordinates held fixed in the free-energy calculation are changed by a small amount and the free-energy calculation is repeated. The resulting free-energy difference is used to obtain a transition probability for the change of the c.m. and classical-particle configuration according to the familiar MC importance sampling scheme. A variation of this combination of staging and importance sampling is to move all primary chain particles and the classical particles subjected to an effective potential determined by averaging over secondary chain configurations. This procedure may be particularly appropriate for fluids.

In this paper the staging algorithm has been tested for the case of a low-density hard-sphere system. The main reason for studying this particular system was the possibility of a comparison of a MC simulation of an electron solvated in a fluid to analytical results obtained for the same model system by means of self-consistent integral equations.[13] These calculations predict a localization of the electron in the hard-sphere solvent in the density range considered in Secs. IV and V. However, in this pa-

per the rigid system is investigated first in order to separate the difficulties of simulating a quantum particle in a complicated potential from the process of annealing the distribution of classical particles. A significant result is the dramatically different behavior of an electron in a rigid disordered system in comparison to an electron in a lattice. It is likely that this effect is related to the phenomenon of Lifshitz's deep traps[21] and the presence of low-energy tails in electron scattering from impurities in semiconductors.[22,23] Moreover, the low-temperature conductivity of such systems has been found to be much lower than in the pure system; this phenomenon is known as weak localization.[24] The question of how the electron will respond when the configuration of hard spheres is allowed to anneal via one of the procedures mentioned above remains to be investigated.

[1]R. P. Feynman and A. R. Hibbs, *Quantum Mechanics and Path Integrals* (McGraw-Hill, New York, 1965); R. P. Feynman, *Statistical Mechanics* (Benjamin, New York, 1972).
[2]D. Chandler and P. G. Wolynes, J. Chem. Phys. **74**, 4078 (1981); N. S. Schweizer, R. M. Stratt, D. Chandler, and P. G. Wolynes, J. Chem. Phys. **75**, 1347 (1981).
[3]H. De Raedt and B. De Raedt, Phys. Rev. A **28**, 3575 (1983); R. A. Friesner and R. M. Levy, J. Chem. Phys. **80**, 4488 (1984).
[4]L. D. Fosdick and H. F. Jordan, Phys. Rev. **143**, 58 (1966); H. F. Jordan and L. D. Fosdick, *ibid.* **171**, 128 (1968).
[5]E. L. Pollock and D. M. Ceperley, Phys. Rev. B **30**, 2555 (1984).
[6]G. Jacucci and E. Omerti, J. Chem. Phys. **79**, 3051 (1983).
[7]R. W. Hall and B. J. Berne, J. Chem. Phys. **81**, 3641 (1984).
[8]M. Parrinello and A. Rahman, J. Chem. Phys. **80**, 860 (1984).
[9]B. De Raedt, M. Sprik, and M. L. Klein, J. Chem. Phys. **80**, 5719 (1984).
[10]R. A. Kuharski and P. J. Rossky, Chem. Phys. Lett. **103**, 357 (1984).
[11]D. Thiwmulai, R. W. Hall, and B. J. Berne, J. Chem. Phys. **81**, 2523 (1984).
[12]J. A. Barker, J. Chem. Phys. **70**, 2914 (1979).
[13]D. Chandler, Y. Singh, and D. M. Richardson, J. Chem. Phys. **81**, 1975 (1984); A. L. Nichols III, D. Chandler, Y. Singh, and D. M. Richardson, J. Chem. Phys. **81**, 5109 (1984).
[14]E. H. Lieb, J. Math. Phys. **8**, 43 (1967).
[15]J. M. Hammersley and N. W. Morton, J. R. Stat. Soc. B **16**, 23 (1954); F. L. McCrackin, J. Res. Nat. Bur. Stand. Sect. B **76**, 193 (1972).
[16]L. R. Pratt, J. Chem. Phys. **77**, 979 (1982).
[17]D. L. Freeman and J. D. Doll, J. Chem. Phys. **80**, 5709 (1984).
[18]S. Y. Larsen, J. Chem. Phys. **48**, 1701 (1968).
[19]E. Wigner and S. Seitz, Phys. Rev. **43**, 804 (1933).
[20]D. J. Adams, Chem. Phys. Lett. **62**, 329 (1979).
[21]I. M. Lifshitz, Usp. Fiz. Nauk **83**, 617 (1964) [Sov. Phys.—Usp. **7**, 549 (1965)].
[22]B. I. Halperin and M. Lax, Phys. Rev. **148**, 722 (1966).
[23]R. Friedberg and J. M. Luttinger, Phys. Rev. B **12**, 4460 (1975).
[24]G. Bergmann, Phys. Rep. **107**, 1 (1984).